Cite this article
Omoregie AI, Ong DEL, Li PY *et al.* (2024)
Effects of push–pull injection–suction spacing on sand biocementation treatment.
Geotechnical Research **11(1)**: 28–42,
https://doi.org/10.1680/jgere.22.00053

Review Paper
Paper 2200053
Received 13/09/2022; Accepted 11/01/2023
First published online 19/01/2023
Published with permission by Emerald Publishing Limited under the CC-BY 4.0 license.
(http://creativecommons.org/licenses/by/4.0/)

Geotechnical Research

Effects of push–pull injection–suction spacing on sand biocementation treatment

1 **Armstrong Ighodalo Omoregie** PhD
Post-doctoral Researcher, Department of Water and Environmental Engineering, School of Civil Engineering, Faculty of Engineering, Universiti Teknologi Malaysia, Johor Bahru, Malaysia (Orcid:0000-0002-6356-9638) (corresponding author: ioarmstrong@utm.my)

2 **Dominic Ek Leong Ong** PhD
Senior Lecturer, School of Engineering and Built Environment, Griffith University, Brisbane, Australia (Orcid:0000-0001-8604-8176)

3 **Phua Ye Li** MEng
Civil Engineer, Southern Regional Office, Sarawak Public Works Department, Kuching, Malaysia

4 **Nurnajwani Senian** MEng
Civil Engineer, Coastal Second Trunk Road Unit, Sarawak Public Works Department, Kuching, Malaysia (Orcid:0000-0002-6541-5552)

5 **Ngu Lock Hei** PhD
Senior Lecturer and Associate Dean for Curriculum Enhancement and Accreditation, School of Chemical Engineering and Science, Faculty of Engineering, Computing and Science, Swinburne University of Technology Sarawak Campus, Kuching, Malaysia (Orcid:0000-0003-2970-555X)

6 **Annette Esnault-Filet** MEng
Project Manager (Research Development), Soletanche Bachy, Paris, France (Orcid:0000-0003-2350-1708)

7 **Khalida Muda** PhD
Professor, Department of Water and Environmental Engineering, School of Civil Engineering, Faculty of Engineering, Universiti Teknologi Malaysia, Johor Bahru, Malaysia (Orcid:0000-0001-7285-7044)

8 **Peter Morin Nissom** PhD
Associate Professor, School of Chemical Engineering and Science, Faculty of Engineering, Computing and Science, Swinburne University of Technology Sarawak Campus, Kuching, Malaysia (Orcid:0000-0002-6514-3921)








The process of ureolysis-driven biocementation is used to improve granular soils. The precipitation of calcium carbonate ($CaCO_3$) crystals results from the reactions of urease generated by ureolytic bacteria and chemical reagents, which strengthen or bind soil particles together. Using a lab-based scaled physical model, this study investigated the influence of selected spacing intervals (107, 214 and 321 mm) on the effectiveness of biocementation through the injection–suction or 'push–pull' approach. Polystyrene moulds were used to create soil specimens. These were then injected with six cycles of treatment solutions at the intervals stated. The compressive strengths and calcium carbonate contents of the biocemented soil specimens were measured after curing. Scanning electron microscopy (SEM), energy-dispersive X-ray spectroscopy (EDS), Fourier transform infrared (FTIR) spectroscopy and effluent analysis (pH and ammonium measurements) were also performed. The biocemented soil specimens with different spacing intervals obtained compressive strengths of 2.53 ± 1.06 to 4.2 ± 2.3 MPa, while the calcium carbonate contents were from 2.78 ± 0.3 to 11.16 ± 1.5%. The elemental compositions and bonding of calcium carbonate precipitates in the biocemented soil were confirmed by EDS and FTIR spectra, while SEM micrographs revealed chip-like and irregular rhombohedral crystal forms. The results demonstrated that injection spacing had an effect on biocemented soil treated by microbially induced carbonate precipitation.

Keywords: biocementation/compressive strength/material structure/soil stabilisation/sustainable development/UN SDG 13: Climate action

Introduction

Due to increased urbanisation and population growth, the globally available land suitable for construction is shrinking (Liu *et al.*, 2022). Cement, which is widely available on the market, is routinely used as a soil stabiliser to increase soil strength and reduce permeability while restricting compressibility (Feng *et al.*,

2020). However, the production of cement has a significant environmental impact due to the high amount of greenhouse gases emitted, such as carbon dioxide (CO_2). As a result, researchers continue to look for alternative binding agents that have a low or no carbon dioxide footprint ('carbon footprint').

Microbially induced carbonate precipitation (MICP) is a new method of soil stabilisation that involves carbonate minerals in the soil matrix (Casas *et al*., 2022). The MICP technique has attracted the interest of researchers all around the world in recent decades due to its potential to improve the engineering properties of granular soil. MICP is a promising alternative to traditional ground improvement binder approaches. This is due to the low mechanical energy created and the low carbon footprint caused by compaction, which results in a more cost-effective and less dangerous environment (Muhammed *et al*., 2021). Despite its popular usage for ground repair, various researchers have shown that MICP can be utilised to treat other practical environmental concerns (i.e. industrial waste water contamination, heavy metal pollution, erosion control and soil liquefaction).

Geological factors regularly influence tunnelling, road construction and ground stabilisation and ground improvement (Choo and Ong, 2020; Peerun *et al*., 2020). Furthermore, the rapid advancement of human activities has resulted in vast volumes of environmental waste and pollution. Thus, in recent decades, engineers have been lured by alternate approaches/methods with zero or reduced carbon footprint for construction purposes (Ojuri *et al*., 2022). MICP is a treatment process used in biocementation to produce inorganic calcium carbonate ($CaCO_3$). Furthermore, it functions as a cementitious (binding) agent, improving the strength and rigidity of granular soil (Omoregie *et al*., 2019). According to evaluation trials, the biocementation process greatly improves the interface shear strength of geo-structures, with an interface efficiency factor of at least 2 and up to 7. It would be useful for friction piles, earth-retaining structures, reinforced slopes and embankments (Mortazavi *et al*., 2021). Calcium carbonate precipitation performance is primarily determined by biological (enzymatic activity), chemical (cementation ingredients and concentration) and physical (soil nature) characteristics (Omoregie *et al*., 2021). Although biocementation technology is gaining popularity, numerous criteria that will contribute to optimal bacterial activity, permitting real-time implementation of the method in a variety of planned procedures, have yet to be standardised (Hadi *et al*., 2022).

MICP activity necessitates the use of ureolytic bacteria to mediate/facilitate carbonate precipitation (Li *et al*., 2021). The ureolysis-driven MICP process involves using urease (EC 3.5.1.5, urea amidohydrolase) to catalyse the hydrolysis of a non-conductive urea molecule to produce 2 mol of ammonium (NH_4^+) (positively charged) ions and 1 mol of carbonates (negatively charged) ions (Omoregie *et al*., 2022) as indicated in Equation I. Microbial urease, which is nickel dependent, can accelerate urea hydrolysis up to 10^{14} times faster than the usual urea hydrolysis process (Singh *et al*., 2017). Urease is an important enzyme secreted by soil microorganisms, although it can also be created through microbial fermentation (Khan *et al*., 2019). The pH rises during the MICP process due to ammonium generation, and ureolytic bacterial cells generate enough metabolic products to react with calcium ions (i.e. calcium chloride ($CaCl_2$)) in the microenvironment to make 1 mol of calcium carbonate, as shown in Equation II. Moreso, Equation III describes the heterogeneous nucleation of calcium ions to the external microbial cell surface.

$$\text{I.}\quad CO(NH_2)_2 + H_2O \xrightarrow{\text{urease}} CO_3^{2-} + 2NH_4^+$$

$$\text{II.}\quad Ca^{2+} + CO_3^{2-} \rightarrow CaCO_3$$

$$\text{III.}\quad Ca^{2+} + \text{cells} + CO_3^{2-} \rightarrow \text{cells} - CaCO_3$$

Urease is a well-known enzyme that is employed in a wide range of industrial applications, such as drinks, fertilisers, medical sensor kits and pharmaceutical products (Bracco *et al*., 2019; Khan *et al*., 2019; Singh *et al*., 2017). However, urease from a microbe (i.e. *Sporosarcina pasteurii* and *Lysinibacillus sphaericus*) or a plant (i.e. watermelon and jack bean) has piqued the interest of the construction industry interest in bioprecipitation of calcium carbonate as a binder agent for soil solidification. Ureolytic bacteria are noteworthy in that they choose substrates (e.g. urea) for development and survival in the environment (Mekonnen *et al*., 2019). Ureolysis-driven MICP requires microbial agents to act as a nucleation site for calcium carbonate crystallisation to happen.

The growing need to develop marginal ground for specific construction projects has prompted civil engineers and biotechnologists to investigate novel sustainable soil improvement approaches (Muhammed *et al*., 2021). Many studies have successfully used the MICP treatment procedure to improve the unconfined compressive strength (UCS) and other engineering parameters of granular soils (Bang *et al*., 2001; DeJong *et al*., 2010; Stocks-Fischer *et al*., 1999; Whiffin *et al*., 2007). Biocementation through pressure injection treatment is believed to be the most prevalent method used by MICP scholars for soil improvement. This approach necessitates the injection of a cementation solution into the soil specimen, either with or without bacterial colonies. Unwanted retention or adhesion of bacteria and cementation at injection points limit the volume of the solution moving through the entire soil matrix during MICP treatment of the soil (Mujah *et al*., 2017). This can have an impact on the calcium carbonate contents, permeability and strength.

The impediment of treatment fluid flow during treatment due to clogging, as well as the uneven distribution of calcium carbonate precipitation along the treated soil matrix, is a significant barrier to MICP technology. This is because the homogeneity of calcium

carbonate precipitates has a major influence on the treated soil sample, UCS and soil stability (Ahenkorah *et al*., 2020, 2022). To address this issue, several researchers proposed reducing the pH of the cementation solution, varying the concentration of the cementation solution and utilising a lower-salinity solution (Cheng *et al*., 2019; Gomez *et al*., 2016a; Lee *et al*., 2019a). Changing the injection pattern, such as using numerous stages of injection treatment, may also be beneficial in preventing the formation of clogs at injection wells/points (Gowthaman *et al*., 2019; Mohsenzadeh *et al*., 2022; Muhammed *et al*., 2021).

Many studies have demonstrated that many biogeochemical parameters (e.g. temperature, pH levels, bacterial cell fixation, cementation concentration, freezing and thawing, soil type and reaction and curing conditions) have a significant impact on the performance of the soil biocementation treatment (Gowthaman *et al*., 2020; Harkes *et al*., 2010; Li *et al*., 2015; Peng and Liu, 2019; Zhao *et al*., 2014). Since MICP can serve as an alternative ground improvement treatment method, in this research, the effect of injection spacing on soil biocementation is studied in greater detail. The injection treatment mould specimens had spacing distances of 107 mm (5D), 214 mm (10D) and 321 mm (15D), where D is the diameter of the injection well. The performance of MICP was determined based on compressive strength, the mass of calcium carbonate contents, morphological and elemental compositions, functional group compound behaviour and urease activity of effluent samples through pH and ammonium measurements.

Materials and methods

Ureolytic microorganism

The ureolytic microorganism used in this study was *S. pasteurii* (DSM 33 strain) purchased from the Leibniz Institute DSMZ – German Collection of Microorganisms and Cell Cultures (Braunschweig, Germany). A freeze-dried culture stock of *S. pasteurii* was rehydrated in sterile tryptone soya agar (40 g/l, Oxoid Thermo Scientific Microbiology) and subcultured until pure bacterial colonies were obtained. The revived bacterial cells were then grown on a sterile cultivation medium containing analytical-grade nutrient broth (13 g/l, HiMedia Laboratories Pvt. Ltd) and urea (20 g/l, Merck Sdn Bhd) at 32°C. The bacteria were aseptically grown overnight under aerobic batch conditions in an incubator (MMM Incucell) and later harvested during the late exponential growth phase. The bacterial cultures were kept in the fridge (4°C) for the subsequent experiments and not stored longer than a month.

Cementation solution

The cementation treatment solution used for the biocementation test consisted of tryptic soy broth (3 g/l, Sigma-Aldrich Co. LLC), hydrated calcium chloride (0.75 M, Sigma-Aldrich Co. LLC), urea (0.75 M, Bendosen Laboratory Chemicals) and ammonium chloride (10 g/l, HiMedia Laboratories Pvt. Ltd). The tryptic soy broth and ammonium chloride were dissolved in deionised water and then sterilised in an autoclave machine (Hirayama autoclave HV-110L) at 121°C. The remaining chemicals (urea and calcium chloride) were added to the sterile solution after autoclaving to prevent any unwanted chemical decomposition that may occur during autoclave conditions (Omoregie *et al*., 2017). The chemical solution was later placed inside a biological safety cabinet and ultraviolet-sterilised for at least 15 min before being used. All the chemicals and nutrients used in this study were of analytical grade (high purity).

Sand mould preparation

The sandy soil used in this experiment was attained from Batu Kawah Sand Quarry (Phua Kheng Heng Sdn Bhd). The particle size distribution of the soil ranged from fine sand (0.075 mm) to fine gravel (4.75 mm) as summarised in Table 1 and Figure S1 in the online supplementary material.

The soil utilised in this study is classed as poorly graded sand (SP) by the Unified Soil Classification System (ASTM, 2020). Because of their inertness and ease of sample extraction, polystyrene boxes were utilised as the single-use moulds in the experiment. By cutting the foam with a knife, the sample can be easily extruded from the foam. Furthermore, several researchers have reported employing polystyrene boxes as soil columns (Xiao *et al*., 2020). After that, the sand was compacted into a clean polystyrene mould with interior dimensions of 444 mm (L) × 278 mm (W) × 165 mm (H) and a maximum sand density of 35%. The relative density of soil after placement in the mould was 1400 kg/m^3.

The polystyrene specimens used in this study were compacted into five different layers with soil for better retention between soil layers. Before compaction, the soil was mixed with 1000 ml bacterial cultures (biomass concentration of 1.39×10^7 colony-forming units/ml and urease activity of 11.6877 mM urea hydrolysis/min) as shown in Figure S2 in the online supplementary material. The bacterial cultures were mixed with sand and placed in the mould rather than injected to examine the flow of the cementation fluid rather than the bacterial culture. Following earlier studies, this strategy was chosen (Soon *et al*., 2014; Zhao *et al*., 2014). The injection method of the bacterial

Table 1. Particle size specification details of the sand in this study

Characteristic	Value
Soil classification	SP
D_{10}: mm	0.125
D_{50}: mm	0.210
D_{60}: mm	0.240
Coefficient of uniformity, C_u	1.92
Coefficient of curvature, C_c	1.20
Specific gravity, G_s: kg/m^3	2.670
Maximum dry density, $\rho_{d\ max}$: Mg/m^3	1.640
Minimum dry density, $\rho_{d\ min}$: Mg/m^3	1.27
pH value	6.29

solution, on the other hand, is also another accepted approach often utilised for soil biocementation.

Each of the layers was carefully compacted by using a tamper to a height of 3 cm, which was 35% of the maximum density of the sand. Poly(vinyl chloride) (PVC) pipes with a diameter of 21.4 mm (perforated hole ø = 10 mm) served as the injection treatment pipes (Figure S3 in the online supplementary material). All four pipes were inserted vertically before the compaction of the bacterial culture mixed sand. Each pipe had a bottom end cap and a perforated side with two columns of holes. The injection pipes were then encased in Scotch pads to prevent sand particles from entering the injection pipes. If sand particles get into the pipes, they will eventually cause bioclogging and impede the distribution of the treatment fluid. After that, rubber pipe insulators were installed at each pipe section to avoid cementation solution up-flow and the hydraulic pressure phenomenon of sand around the injection pipes during the treatment process (Figure S4 in the online supplementary material). By adjusting the pressure in the pressure vessel between 0.02 and 1.00 bar, the injection rate was kept constant at 1 l/h. To create a push–pull effect, an air compressor was attached to the injection wells and a vacuum pump was linked to the extraction wells. This was done to aid in the movement of treatment fluids (e.g. bacterial cells and cementation solution) and to eject waste water effluents by exerting pressure.

Biocementation treatment

A two-stage injection biocementation treatment method was used in this study to test the influence of injection–suction well spacing of MICP treatment on the mechanical properties of soil as shown in Figure S5 in the online supplementary material. It is noted that the fresh solutions were injected, and the effluent was discarded, whereas only fresh solution was injected for the next cycles. The injection spacings were designated as 5D, 10D and 15D (see Table 2), where D is the well outer diameter measuring 21.4 mm. The pore volume of the sand was 0.27. After a 6 h retention period of the bacterial fixation process, injection of cementation solution was initiated, which lasted for 72 h. This retention period of the bacterial cells was selected because the duration was sufficient for ionic strength on microbial transport. There was a total of six treatment cycles (twice a day) of the cementation placement through the injection wells. For each batch treatment, 5 l of the cementation solution was injected into the mould specimens.

The injection rate was maintained at approximately 1 l/h (i.e. 0.02–1.00 bar) for the influent pressure vessel. The suction pressure from the vacuum pump was maintained at 0.05 bar throughout the entire treatment process to prevent over-saturation on the top surface of the sample. The treatment fluids in the influent pressure vessel were periodically shaken (every 15 min) to prevent sedimentation from occurring. At the end of the treatment, distilled water (three times the sample volume) was injected into the treated moulds to rinse out unwanted chemical residue from the soil matrix (Gowthaman *et al.*, 2019). The polystyrene moulds were then carefully cut using a penknife and taken out. The moulded treated samples were subsequently allowed to cure under the same atmospheric condition as the MICP treatment condition for 7 days before being subjected to further analyses (compressive strength, calcium carbonate content and mineralogical analysis).

Table 2. Selected injection pipes with spacing distance

Sample	Distance between wells: mm
5D	107
10D	214
15D	321

Compressive strength determination

The surface strength and compressive strength of the biocemented sand samples were determined through penetration resistance tests and UCS measurements. Surface strength measurement was carried out using a calibrated pocket penetrometer (ELE International, 38-2695). This is a simple, portable device that is used to predict the penetration resistance of the top layer (5 mm depth) of the soil specimen. Also, the surface strength served as an economical method for evaluating the surface strength distribution at various locations of the consolidated soil specimens. The surface strength was determined by pushing the tip of the penetrometer onto the biocemented soil to a depth of approximately 6.35 mm (0.25 inches). The measurement was recorded when the samples were completely penetrated up to a depth of 6.35 mm. The penetrometer has a maximum reading value of 700 pounds per square inch (4.83 MPa).

The biocemented sand specimens were also subjected to a UCS test, which is used to measure the axial compressive stress. Parts of consolidated soils treated with different injection spacings were cored through at selected locations to obtain cylindrical cores for the UCS test as shown in Figure S6 in the online supplementary material. To obtain cylindrical samples for UCS testing, the trimming process was used. The samples were meticulously cut into smaller amounts using a chisel and then carefully trimmed to meet the standard size of a cylinder for testing as specified by BS 1377-7:1990 (BSI, 1990). Precaution was taken when handling the samples, as the sample might be fragile in certain locations, in particular near the suction wells. The samples were cored into cylinders (diameter of 50 mm and height of 100 m) and tested with a universal testing machine (GT-7001-L) with a maximum load of 50 kN and a loading speed of 1 mm/min to record the stress (kPa) level.

Mass of calcium carbonate content

After performing the compressive strength tests, gravimetric acid washing was used to measure the mass of the calcium carbonate content in the biocemented sand specimens. The calcium carbonate content is also referred to as the cementation level of MICP-treated soil specimen determined. The amount of calcium

carbonate precipitated within the samples was determined by washing them with hydrochloric acid (HCl) to dissolve the calcium carbonate. The samples in Whatman filter papers (11 µm pore size) were placed in sterile glass funnels as shown in Figure S7 in the online supplementary material. Later, 2 M hydrochloric acid was poured slowly into the filter paper to dissolve the calcium carbonate and later washed with sterile deionised water. The samples were then oven-dried at 60°C for 4 h before being subjected to acid wash. The difference in the two masses of the sand (before and after acid wash) was determined. The weight (mass) of calcium carbonate before and after being subjected to oven drying were used to estimate the calcium carbonate content as shown in the following equation:

$$\text{calcium carbonate content } (\%) = \frac{\text{mass of calcium carbonate}}{\text{mass of the oven-dried specimen} - \text{mass of calcium carbonate}} \quad (1)$$

Scanning electron microscopy–energy-dispersive X-ray spectroscopy analysis

A benchtop advanced microscope (TM4000Plus II, Hitachi Ltd) was used to determine the morphological, topographical and elemental compositions of the crystals formed in sand particles that were subjected to MICP treatment. The scanning electron microscopy (SEM) analysis was performed at an accelerating voltage of 15 kV and magnifications of ×100 and ×250. Energy-dispersive X-ray spectroscopy (EDS) was used to establish the elemental composition and concentration of the tested biocemented sand samples.

Fourier transform infrared analysis

For Fourier transform infrared (FTIR) spectroscopy to determine the functional groups (i.e. C–O bonds) of the crystal formed in the biocemented soil specimens after MICP treatment, an FTIR spectrometer was used (IRAffinity-1, Shimadzu Corporation, Kyoto, Japan). An estimated 1 mg of the biocemented soil sample was mixed with 100 mg of potassium bromide powder in an agate mortar (Achal and Pan, 2014). The contents were then carefully ground within a clean agate pestle until pellets with the desired texture were obtained for FTIR spectroscopy. FTIR spectral scanning of each sample was carried out at wave numbers from 4000 to 400 cm^{-1} with the error range of the analytical method set as ±0.005 cm^{-1} (Li *et al.*, 2013). FTIR spectroscopy functions by detecting the vibrational features of diverse functional groups in organic molecules and then developing a unique molecular fingerprint spectrum (Khui *et al.*, 2021; Wang *et al.*, 2015).

Effluent pH measurement and ammonia concentration

The analysis of the effluent collected during the MICP treatment is a crucial indication of the process occurring in the sand sample. The effluents from the mould specimens were collected during the MICP treatment to measure the pH values and ammonium concentrations. These measurements were conducted as indicative parameters of the urease activity during MICP treatment. A volume of 50 ml of the discharged effluent was collected in sterile plastic centrifuge tubes for pH measurement (SevenEasy, Mettler Toledo pH meter with a precision of 0.01). The 50 ml effluent samples were suspended in a centrifuge machine (Eppendorf, 5804R) at 10 000***g*** for 1 min before the ammonium content was filtered, collected and determined. The collected supernatants were then subjected to ammonium measurement using the phenate method described by Park *et al.* (2009). Ammonia reacts with phenol to form indophenol in the presence of alkali and an oxidising agent. This method is suitable for accurately measuring ammonium concentrations from 0.02 to 2 mg ammonium ions/l (Greenberg *et al.*, 1992). In brief, 10 ml of samples was placed into clean universal bottles and carefully mixed with 0.4 ml of phenol solution, 0.4 ml of sodium nitroprusside and 1.0 ml of the oxidising solution (containing 25 ml of sodium hypochlorite (5%), 200 g/l trisodium citrate and 10 g/l sodium hydroxide). The analysis was conducted at room temperature (24 ± 2°C), and the capped universal bottles containing the mixture solutions were then stored in subdued light conditions for 60 min to allow the chemical reaction to occur. At the end of the incubation, the mixture solutions in the universal bottles turned blue at respective concentrations. The ammonia concentration was determined by measuring the absorbance of indophenol using a spectrophotometer (Genesys 20, Thermo Fisher Scientific) at 640 nm. The measured absorbance of indophenol from the spectrophotometer and calibration curve obtained from several ammonium chloride concentrations as a standard was used to plot a graph of absorbance against ammonia concentration. The slope of the linear correlation was then converted to urease activity by multiplying it by a factor of 0.5, previously derived by Whiffin (2004).

Results and discussion

Compressive strength

The effect of injection spacing on MICP efficiency was evaluated after soil biocementation had been completed and the moulds had entirely hardened, as shown in Figure 1. MICP was applied to the 5D, 10D and 15D mould specimens by injection through PVC pipes spaced 107, 214 and 321 mm apart from the opposing

Figure 1. Sand specimen after biocement treatment with bacterial cultures and cementation solution

suction pipes, respectively. Table 3 shows the compressive strength testing of the soil specimens following biocementation.

For the surface strength obtained through pocket penetrometer tests, 5D, 10D and 15D specimens recorded average strength values of 2.53 ± 1.06 MPa (standard deviation (std. dev.) = 1.055, variance = 1.113, root mean square = 2.72 and sum of squares = 12.246), 2.82 ± 0.82 MPa (std. dev. = 0.892, variance = 0.796, root mean square = 2.943 and sum of squares = 8.756) and 3.42 ± 1.13 MPa (std. dev. = 1.126, variance = 1.268, root mean square = 3.582 and sum of squares = 13.956), respectively. On the other hand, the UCS tests indicated that the obtained results for the samples (5D, 10D and 15D specimens) were 2.57 ± 1.5 MPa (std. dev. = 1.508, variance = 2.274, root mean square = 2.849 and sum of squares = 4.548), 3.12 ± 1.17 MPa (std. dev. = 1.178, variance = 1.389, root mean square = 3.319 and sum of squares = 2.778) and 4.2 ± 2.3 MPa (std. dev. = 1.508, variance = 2.274, root mean square = 2.849 and sum of squares = 4.548), respectively.

The data also illustrate that the soil biocemented core (15D) that had a spacing of 321 mm produced the highest compressive strength, while the column at 107 mm spacing (5D) resulted in the lowest compressive strength. The increased core spacing enhanced the retention time of cementation fluid at the pore between the sand particles, allowing for more time for calcium carbonate crystals to form before they were transported to the extraction wells.

Analysis of variance (Anova) and the post hoc Tukey HSD test revealed no significant changes in surface strength for specimens treated at different spacing distances (P-value = 0.541, F-statistic = 0.681, sum of squares = 4.072, degrees of freedom = 2, mean square = 2.036). Furthermore, Anova and the post hoc Tukey honestly significant difference (HSD) test revealed no significant changes in surface strength for specimens treated with different spacing distances (P-value = 0.116, F-statistic = 2.304, sum of squares = 4.882, degrees of freedom = 2, mean square = 2.441). The P-value is related to the one-way Anova F-statistic, which is more than 0.05, indicating that the treatments (5D, 10D and 15D) are not significantly different at that level of significance.

The strength of these cores increased towards the suction wells and decreased near the injection wells. Nevertheless, all three tested cores with different injection spacings demonstrated that the area beyond the injection pipes resulted in improved compressive strength. As cementation fluid travelled from injection wells to suction wells, crystals of calcium carbonate began to form and became adhered to the sand particles. As a result, more calcium carbonate was formed and the sand near the suction well had a higher compressive strength. This may likely be due to the distribution of calcium carbonate content in the soil columns.

Table 3. Surface strength and UCS measurements of the biocemented sand samples

Specimen	Surface strength: MPa	UCS: MPa
5D	2.53 ± 1.06	2.57 ± 1.51
10D	2.82 ± 0.82	3.12 ± 1.17
15D	3.42 ± 1.13	4.2 ± 2.3

The use of a pocket penetrometer and the UCS test to assess soil cores treated by MICP treatment has been widely documented in the literature (Cheng and Cord-Ruwisch, 2012; Whiffin, 2004). The UCS test, on the other hand, is typically employed after the soil biocementation process to quantify the axial stress applied to the subjected tested specimen along a longitudinal axis (Omoregie *et al*., 2021). It offers a better understanding of the strength homogeneity inside the tested cylinders. As a result, both compressive strength tests were chosen for this investigation to allow for a broad comparison.

Prior to the strength test, calcium carbonate content determination and other mineralogical analyses, the MICP-treated samples were allowed to cure for 7 days. This was to allow bacterial cells and urea to remain and complete the enzymatic and biochemical activities. This may allow for additional biocalcification. Furthermore, the 7-day interval serves as the drying phase for the MICP-treated sample. However, this may be a significant disadvantage of the MICP technique because the treatment may be time consuming or costly for field-scale applications. As a result, this is a variable (treatment time) that can be optimised in future trials.

The surface strength and UCS test data indicated a positive trend, supporting the concept that the injection spacing can alter soil strength and stiffness following MICP treatment. The two-stage injection approach is appropriate for restricting bacteria to the soil before injecting the cementation solution into soil columns (Gowthaman *et al*., 2019). Despite this, only three injection spacings were evaluated in the laboratory. However, the results show that it is critical to optimise the spacings of the injection pipes in the samples to achieve optimal cementation distribution and greatly improved biocemented soil. Because of the particle-to-particle contact mechanism, the effect of MICP treatment on soil mechanical response varies depending on compressive strength and calcium carbonate content (Rahman *et al*., 2020). This indicates the reason why the calcium carbonate content after the strength test was tested to determine if there is a correlation between the two analyses.

Mass of calcium carbonate content

The amount of calcium carbonate generated within the soil matrix can have an impact on the mechanical properties of biocemented treated soil. Determining the bulk of calcium carbonate content following soil biocementation treatment is therefore crucial. Table 4 shows the calcium carbonate content of biocemented soil specimens treated with varied spacings (5D, 10D and 15D). The highest calcium carbonate content was at the bottom layer (4.90 ± 1.52 to 11.16 ± 15%) of all soil moulds irrespective of the

Table 4. Calcium carbonate content determination after soil biocementation treatment

Sample	Top layer: %	Middle layer: %	Bottom layer: %
5D	2.78 ± 0.3	3.70 ± 0.6	4.90 ± 1.52
10D	3.26 ± 0.3	4.41 ± 0.5	7.23 ± 1.9
15D	6.24 ± 0.7	7.69 ± 0.5	11.16 ± 15

injection spacings. On the other hand, the measured lowest calcium carbonate content was at the top layer of the soil moulds (2.78 ± 0.3 to 6.24 ± 0.7%). More so, out of all tested injections, a spacing of 321 mm (15D sample) produced the highest calcium carbonate content, while the specimen with a spacing distance of 107 mm (5D) had the lowest calcium carbonate content (Table 4).

The statistical analysis using Anova revealed significant differences in the surface strength values for the calcium carbonate contents at the top layer of the soil columns (P-value = 0.0002, F-statistic = 50.403, sum of squares = 21.115, degrees of freedom = 2 and mean square = 10.558). The post hoc Tukey HSD test revealed significant differences when sample 5D (std. dev. = 0.280, variance = 0.078, root mean square = 2.792 and sum of squares = 23.39) and sample 10D (std. dev. = 0.346, variance = 0.119, root mean square = 3.268 and sum of squares = 32.057) were compared with sample 15D (std. dev. = 0.656, variance = 0.430, root mean square = 6.266 and sum of squares = 117.79). When the values of 5D and 10D were examined, however, there was no significant difference. The statistical analysis using Anova revealed significant variations in the surface strength values for the calcium carbonate contents at the mid-layer of the soil column (P-value = 0.0004, F-statistic = 39.1494, sum of squares = 27.243, degrees of freedom = 2 and mean square = 13.621). The post hoc Tukey HSD test revealed significant differences when samples 5D (std. dev. = 0.636, variance = 0.402, root mean square = 3.722 and sum of squares = 41.579) and 10D (std. dev. = 0.574, variance = 0.329, root mean square = 4.438 and sum of squares = 59.090) were compared with sample 15D (std. dev. = 0.559, variance = 0.312, root mean square= 7.700 and sum of squares = 177.879). When the values of 5D and 10D were examined, however, there was no significant difference. The statistical analysis using Anova revealed that there were significant variations among the surface strength values for the calcium carbonate contents at the bottom layer of the soil column (P-value = 0.009, F-statistic = 11.276, sum of squares = 60.061, degrees of freedom = 2 and mean square = 30.031). The post hoc Tukey HSD test revealed that only when sample 5D (std. dev. = 2.749, variance = 7.561, root mean square = 4.379 and sum of squares = 22.682) was compared with sample 15D (std. dev. = 5.712, variance = 32.628, root mean square = 9.722 and sum of squares = 97.886) were significant differences observed. When sample 5D or 15D values were compared with sample 10D values, no significant difference was seen (std. dev. = 3.917, variance = 15.343, root mean square = 6.396 and sum of squares = 46.030).

The results showed that the injection treatment method utilised for soil biocementation with various spacings affects the calcium carbonate content. The calcium carbonate formation reacted as it moved towards the suction regions during the initial MICP injection treatment due to a positive hydraulic gradient from the injection wells to the suction wells. Table 4 shows that as the treatment solution moves from the injection regions to the suction regions, more calcium carbonate content is generated away from the injection sections. This result is critical for understanding the soil biocementation process because it inhibits bioclogging formation at injection wells, which is a common concern during MICP treatment. The data also revealed that the cementation did not change significantly among the three layers (top, middle and bottom) of the treated soil specimens. This could imply that there were enough active bacterial cells in the soil matrix to facilitate ureolysis. The results also suggest that the amount of calcium carbonate precipitate decreases with the distance from the injection point to the suction point, which can be attributed to the restriction of treatment solution flow caused by bioclog formation, which influences the outcome of the MICP process (Sidik *et al.*, 2014). To ensure efficiency in the MICP process, it is recommended to inject or immobilise the bacterial cells with the soil before the subsequent daily injection of cementation solution (Gowthaman *et al.*, 2019). When too many bacterial cultures are injected or introduced into the soil sample, it may affect the treatment efficiency.

The non-uniformity of the UCS in the soil samples is caused by the varying amounts of precipitation generated after MICP injection at various places along the treatment flow path. This was caused by unequal cementation solution transportation further away from the injection wells (Gomez *et al.*, 2016b). By adjusting the well spacing, precipitation may be increased at the injection and suction zones, which will assist limit the production of undesired bioclogs. Other researchers such as Harkes *et al.* (2010) have proposed lowering the flow rate of the treatment solution (cementation solution and bacterial culture) to improve the drawback (non-uniformity of calcium carbonate distribution) affecting MICP performance, while others have suggested a waiting period to allow proper attachment of bacterial cells to the soil before further injection (Al Qabany *et al.*, 2012). However, this study showed that the distance between the wells (injection and suction) could also significantly influence the overall performance of MICP. Another opinion worth considering is the concentrations (0.75 M) of urea and calcium chloride used in this study. It was previously reported that using an appropriate concentration of cementation reagents caneffectively improve the outcome of MICP and reduce heterogeneous crystal formation at the soil contact spots (Gowthaman *et al.*, 2019; Mujah *et al.*, 2017).

SEM–EDS analysis

SEM–EDS analysis was undertaken to examine the effect of biocementation treatment with varying spacings on the microstructure of the MICP-treated soil particles, as shown in Figures 2–4 and Table 5. Figure 2(a) shows that the soil particles in the 5D sample were connected, with only a few crystal forms found within the sand particle. The SEM micrograph (Figure 3(a))

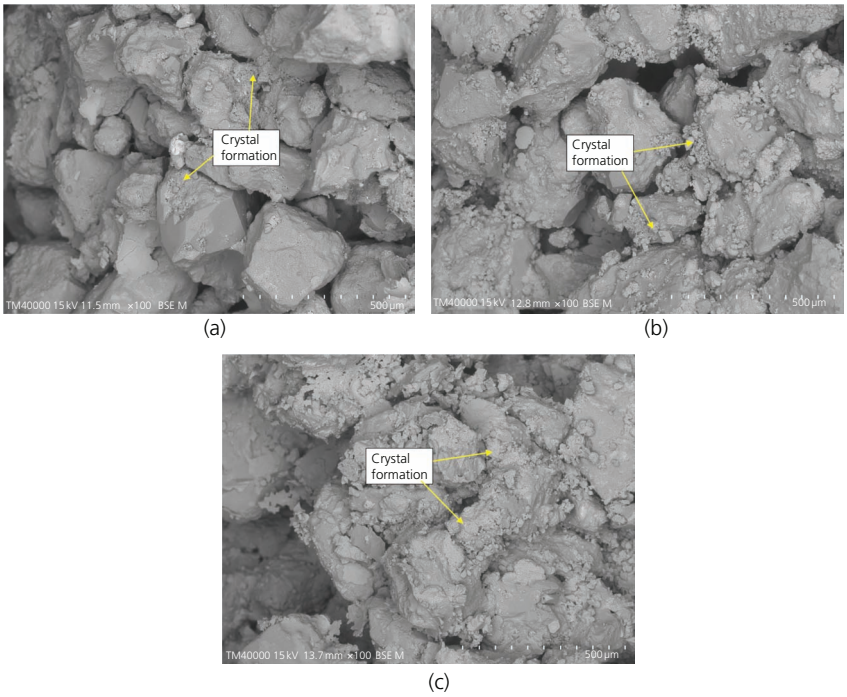

Figure 2. SEM micrographs at ×100 magnification showing sand particles after biocementation treatments with (a) 5D, (b) 10D and (c) 15D injection pipes

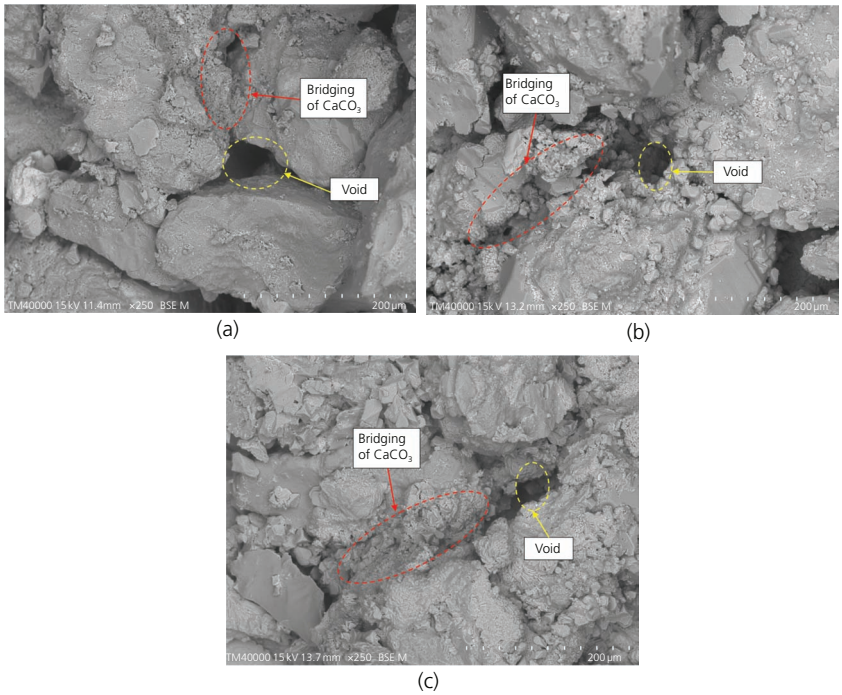

Figure 3. SEM micrographs at ×250 magnification displaying calcium carbonate formations at interparticle contact bonding for sand particles treated with (a) 5D, (b) 10D and (c) 15D injection pipes

of the 5D sample, on the other hand, showed interparticle bonding of sand particles with crystal formations with rough surfaces.

When compared with the 5D sample, the SEM findings for the 10D sample in Figures 2(b) and 3(b) revealed that there were

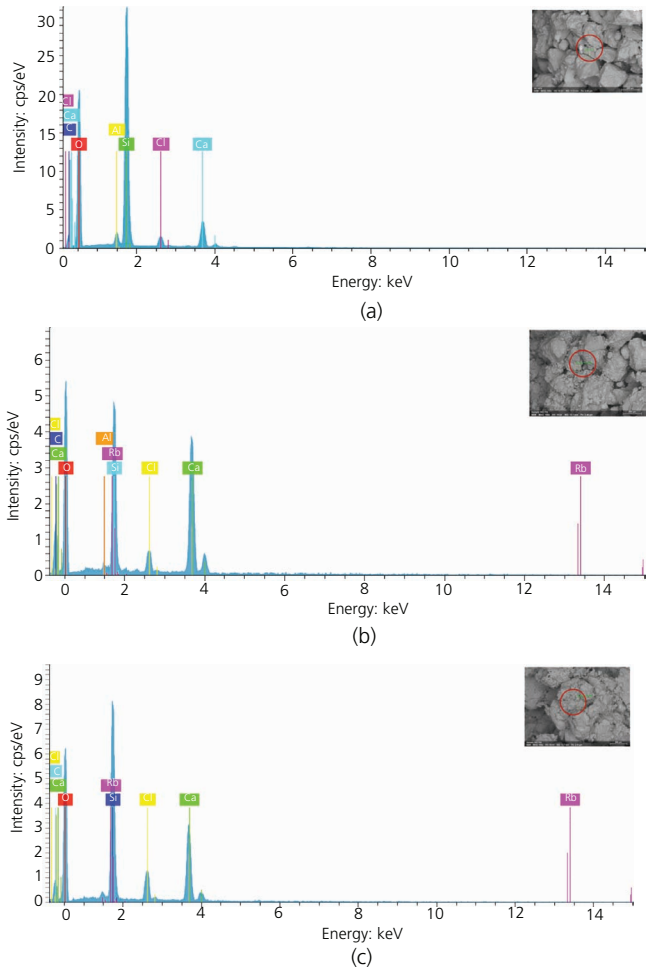

Figure 4. EDS analysis showing elemental compositions of sand particles treated with (a) 5D, (b) 10D and (c) 15D injection pipes. cps, counts per second

Table 5. EDS analysis identifying the elements in the sand specimens after MICP treatment

Element	5D sand mass: %	10D sand mass: %	15D sand mass: %
Oxygen (O)	72.80	67.02	69.45
Silicon (Si)	33.28	10.59	20.23
Carbon (C)	16.27	20.86	16.14
Calcium (Ca)	8.35	22.50	16.54
Chlorine (Cl)	2.05	2.12	4.85
Aluminium (Al)	1.73	0.42	0.00
Rubidium (Rb)	0.00	2.99	0.00

more crystals attached to the sand particles. At the soil contact locations, numerous crystal clusters with rough surface morphologies developed. When compared with the 5D sample, the 10D sample exhibited fewer pore regions within the soil matrix, while the 15D sample had no apparent pore regions inside the soil matrix. The presence of significant spaces between the soil matrix indicates that less cementation occurred in sample 5D, making it more sensitive to permeability as compared with the other improved soil samples. This finding also suggests that MICP injection treatment with varying spacings for soil improvement has a significant impact on crystalline formation. The extent of calcium carbonate crystal formation and the distribution of cementation influence sand permeability after the MICP treatment (Chen *et al.*, 2018).

The results in Figures 2(c) and 3(c) clearly show that the sand particles were fully connected with crystal formations and there were several large clusters of crystals formed at the contact regions of the soil. A similar observation was reported by Gowthaman *et al.* (2021), who reported observing high contents of calcium carbonate formation and larger clusters between soil particles in their study on the influence of acid rain after MICP soil treatment. The coating-like layer of calcium carbonate crystals that covered the surface areas of the sand grains observed in this study is similar to those in previous reports (Cheng *et al.*, 2019; Gowthaman *et al.*, 2019). The shapes of biomineral crystals formed after MICP treatment could be influenced by biopolymers or amino acid organic polymers, urease activities and cementation concentration (Cheng *et al.*, 2019).

Calcium carbonate clusters produced at particle contact locations serve an important function in improving soil strength and stability. The abundance of crystal formations on the surface of the sand particle, together with the production of lucid bridges as a connecting point for sand grain particles, is consistent with prior research findings (Cheng and Cord-Ruwisch, 2014; Cheng *et al.*, 2017). Furthermore, the SEM micrographs in Figure 2 revealed that the soil specimens from samples 10D and 15D contained multiple visible chip-like crystal and rhombohedral forms. The smooth surface of the chip-like crystal formations had a ductile feature, whereas the rhombohedral crystal, which was not as prominent or apparent as the chip-like structure, appeared to have rough surfaces.

SEM–EDS analysis is routinely used to determine the calcium carbonate element compositions in soil particles. The EDS elemental compositions of 5D, 10D and 15D biocemented sand particles are shown in Table 5. Furthermore, Figure 4 shows the elemental component spectrum graphs for the samples in accordance with the values reported in Table 5. The elements detected in the biocemented sand samples were oxygen, silicon, carbon, calcium, chlorine, aluminium and rubidium, according to the EDS analysis. The results of EDS analysis in Table 5 and Figure 4 show that oxygen was the most abundant element in all samples in terms of weight and atomic percentage. The elemental concentrations of the biocemented sand samples were also moderate for the 5D (silicon and carbon), 10D (silicon, calcium and carbon) and 15D samples (silicon, calcium and carbon). The remaining components in these soil samples had low or negligible concentrations. Other trace elements (e.g. aluminium and rubidium) are viewed as unimportant due to their low mass or atomic percentages. When comparing the principal elements

discovered in all the biocemented sand samples based on weight percentage, the data from Table 5 indicate that the 5D sample (72.80%) included more oxygen and silicon. Carbon and calcium, on the other hand, were more abundant in sample 10D than in the other treated soil samples. Several MICP researchers have discovered that the crystal precipitates are primarily composed of carbon, oxygen and calcium (Fang *et al*., 2019; García *et al*., 2016; van Paassen, 2011). EDS spectra are also utilised to confirm the presence of calcium carbonate crystals using atomic per cent ratios (García *et al*., 2016). The EDS results for specimen 10D showed higher carbon and calcium levels than the other specimens, which contradicted the SEM findings. This could be due to the mark on the SEM pictures of the location/points where the EDS analysis was performed, which does not reflect the complete biocemented soil sample.

FTIR analysis

FTIR spectroscopy is often used to analyse the composition of functional chemical groups in the treated soil specimens after the MICP process (Achal and Pan, 2014). Figure 5 shows the FTIR spectra of biocemented sand particles treated with different injection spacings. The FTIR results showed that there are four regions that can be grouped as the fingerprint region (600–1500 cm^{-1}), double-bond region (1500–2000 cm^{-1}) triple-bond region (2000–2500 cm^{-1}) and single-bond region (2500–4000 cm^{-1}) (Nandiyanto *et al*., 2019).

FTIR results from the fingerprint region show strong C–Br stretching of halo compounds with wavelengths ranging from 515 to 690 cm^{-1} found in all biocemented sand samples (Figures 5(a)–5(c)). Strong C–H bending peaks were found only in the 5D sample and 15D sample with wavelengths of 752.24 and 759.95 cm^{-1}, respectively. At a wavelength of 906 cm^{-1}, strong C=C bending of monosubstituted alkene and broad CO–O–CO stretching anhydride were detected only in 10D sample and 15D samples. The vibration band from the carboxyl group such as C=O or C=C can be attributed to the organic functional groups from the culture medium used to grow the ureolytic bacterial cells (Han *et al*., 2019).

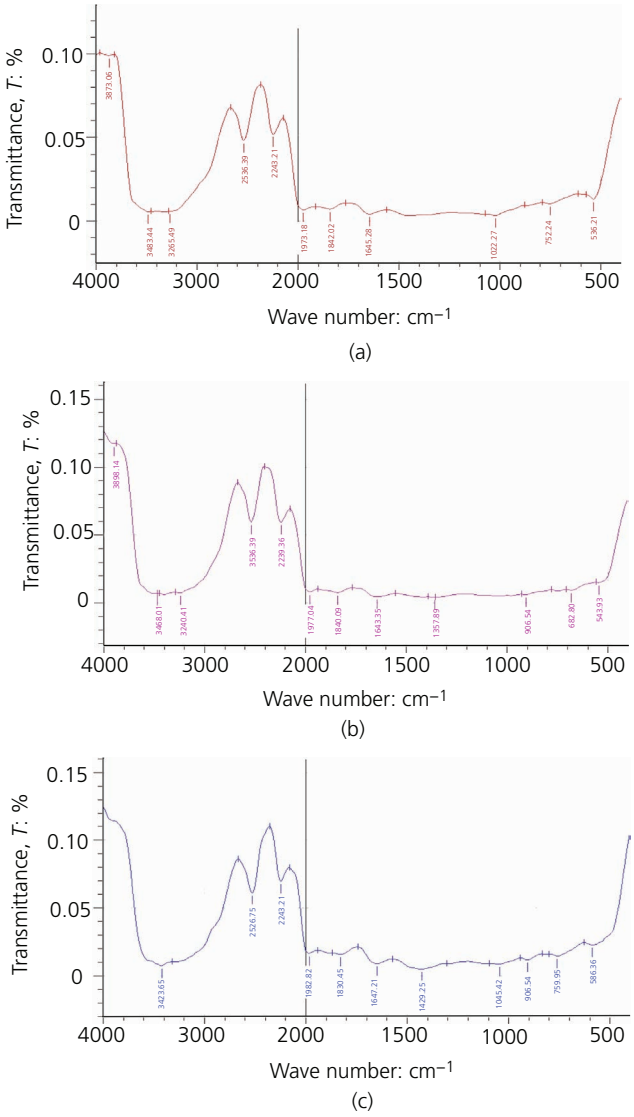

Figure 5. FTIR spectra of biocemented sand particles after treatment with (a) 5D, (b) 10D and (c) 15D injection pipes

Furthermore, strong S=O stretching of sulfonate at a wavelength of 1357.89 cm^{-1} was detected only in the 5D sample, while medium O–H bending of alcohol at a wavelength of 1429.5 cm^{-1} was found only in the 15D sample. The FTIR results showed that strong C=C stretching vibration of a monosubstituted alkene was detected in the 5D sample (Figure 5(a)), 10D sample (Figure 5(b)) and 15D sample (Figure 5(c)) with wavelengths ranging from 1643.35 to 1647.21 cm^{-1}, although there were other identified wavelengths (1830.45–1840.09 cm^{-1}) that fall under the stretching peak band of carbonyl. At wavelength peaks of 1977.04 and 1982.82 cm^{-1}, strong N=C=S stretching of isothiocyanate was found only in the 10D sample and 15D sample. Furthermore, the FTIR spectra showed weak C≡C stretching of a disubstituted alkyne or nitrile in all samples that had wavelengths ranging from 2239.36 to 2243.21 cm^{-1}. The FTIR spectra also identified a medium S–H stretching of thiol in the 5D sample and 15D sample at wavelengths of 2536.39 and 2526.75 cm^{-1}, respectively. Sharp N–H or C–H stretching of primary amine or alkyne was found only in the 5D sample and 15D samples with wavelengths of 3265.49 and 3240.41 cm^{-1}, respectively. Finally, medium/strong O–H or N–H sharp/broad stretching of free alcohol or primary amine was detected at a wavelength ranging from 3423.65 to 3898.14 cm^{-1}, accordingly.

Several MICP scholars have reported biocementation specimens having FTIR spectrum absorption peaks ranging between 700 and 3500 cm^{-1} (Li *et al*., 2013; Srivastava *et al*., 2015; Zhu *et al*., 2016). The strong stretching vibration of the O–H and N–H hydrogen bonds at high peaks (i.e. 3500–3800 cm^{-1}) for the formation of more OH groups are indications of the presence of

organic matter and moisture content (Zhu *et al*., 2016). The FTIR analysis confirmed the presence of calcium carbonate as the main mineral in the microbial sand columns after evaluating the stretching vibrations of the functional groups present in the treated soils (Fang *et al*., 2019).

Effluent pH and ammonium measurement

During soil biocementation, effluent samples were obtained from different locations to track bacterial activity as the injection treatment of the soil columns continued. As a result, pH and ammonium measurements were found to be representations of ureolysis done by bacterial cells (Figure 6). MICP treatment is influenced by both acidic and basic conditions, which may result in reduced compressive strength or calcium carbonate content when compared with those of samples treated in neutral pH settings (Mujah *et al*., 2016). As a result, investigating the pH profile of bacterial activity or ureolytic activity is critical. The results in Figure 6 show a similar trend of the curve lines for samples 5D, 10D and 15D with their respective ureolytic activities. The results show that the values for 5D, 10D and 15D at 0 h were 7.23 ± 0.02, 7.24 ± 0.05 and 8.18 ± 0.05, respectively. The pH measurements showed that all the samples showed lucid and fluctuating lines in response to the injection treatment cycles performed on the soil specimens. The highest pH values observed were 8.30 ± 0.05 (at 24 h), 8.11 ± 0.03 (at 48 h) and 8.20 ± 0.03 (at 48 h) for samples 5D, 10D and 15D, respectively.

The fluctuation of the pH is believed to be caused by urea hydrolysis by urease from bacterial cells, which subsequently leads to an increase in pH and the release of ammonia gas (Li *et al*., 2021). The wells spacings used may have also affected the distribution of the cementation solutions into the columns, thus resulting in varied and fluctuating pH values. During the MICP injection treatment process, the pH values tend to fluctuate with time, suggesting the variation of urea hydrolysis inside the soil column (Al Imran *et al*., 2019). Some scholars have also observed urease activity from collected specimens that were subjected to repeated treatment cycling (Dhami *et al*., 2016). However, it was indicated that not every repetitive injection treatment cycle promotes further urea hydrolysis/urease activity, particularly at a low cementation concentration (i.e. 1 M urea and calcium chloride).

The urease activity results for effluent samples are shown in Figure 7, which shows a trend similar to that observed for the curves in Figure 6 (the pH profile). The data from Figure 7 indicate that urease activities for 5D, 10D and 15D at 0 h were 115.00 ± 3.61, 419.67 ± 6.51 and 479.33 ± 12.50 mM, respectively. The samples had an increment from the initial measurement (first injection cycle) to the next phase of treatment before showing continuous fluctuation for the rest of the treatment cycles. The highest urease activity values obtained at 12 h were 622.00 ± 019.67, 838.67 ± 11.59 and 929.00 ± 6.00 mM for samples 5D, 10D and 15D, respectively. Bacterial enzymatic activity does not cease after biotreatment, resulting in physico-chemical changes in calcite-precipitated soil over time (Sharma *et al*., 2022).

Surprisingly, the highest measurement was obtained in all samples treated with varying spacing distances during the early phase of soil biocementation treatment. The substantial variation in urease activity in effluent samples indicates bacterial activity in the soil. High ureolysis during treatment promotes calcium carbonate precipitation within soil samples, which finally leads to soil solidification (Al Qabany *et al*., 2012; Harkes *et al*., 2010). In the MICP process, changes in pH and urease activity complement calcium carbonate formation. Changes in pH and urease activity help calcium carbonate production in the MICP process. The creation of a significant amount of calcium carbonate crystals correlates with the rise in pH caused by ureolysis due to the release of ammonium ions (Wei *et al*., 2015). The differences in ammonium content produced during MICP are also attributed to the microbial spatial variability and the formulation of the cementation amendment (Martinez *et al*., 2013). Lower

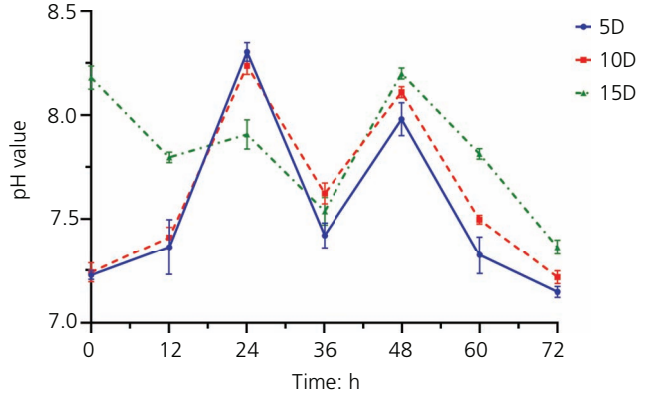

Figure 6. Monitoring of pH activity during soil biocementation treatment

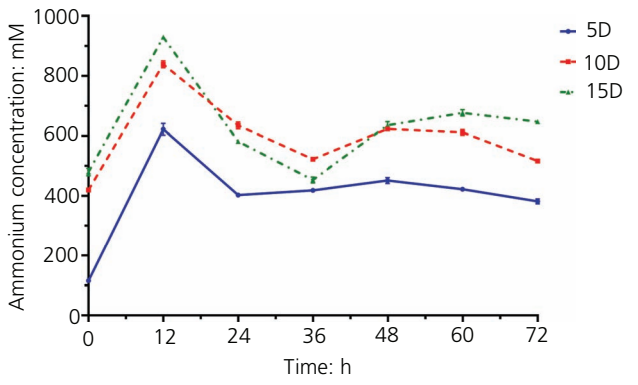

Figure 7. Monitoring of ammonium concentration during soil biocementation treatment

ammonium levels will be released, for example, when lower bacterial cell densities and a lower molar ratio of urea/calcium ions are utilised for MICP treatment.

Figure 7 shows that the spacings of the injection treatment well (PVC pipes) affect MICP treatment. The pH and ammonia levels are related because changes in these levels affect urease activity and calcium carbonate precipitation. In this study, soil columns treated with a 321 mm spacing distance (for the 15D sample) showed higher pH values and urease activity than soil columns treated with 107 mm (for the 5D sample) and 214 mm (for the 10D sample) spacing distances. Furthermore, the 15D sample had more stable and higher pH and urea hydrolysis values, most likely because the cementation solution travelled a long distance, allowing more contact of the cementation solution with the urease enzymes in the sand sample and stable calcium carbonate precipitation to occur. However, because the 10D and 5D samples were separated by a shorter distance, the cementation required a smaller contact area and contact time for the biochemical events to occur, which may have caused the pH and urease activity to be lower than those of the 15D sample.

Biocementation performance

This study discovered that varied injection pipe spacings (107, 214 and 321 mm) during biocementation treatment can alter the generation or distribution of calcium carbonate in soil particles. Calcium carbonate deposition at or near particle-cementing sites would typically cover the soil grains, which would then fill the vacuum spaces. Calcium carbonate filling forms a bridge between sand particles, supporting the matrix and allowing soil solidification to proceed (Lin *et al*., 2016). According to the reported data, the biocementation injection treatment method employed in this investigation successfully cemented the soil samples regardless of the PVC injection spacing distance used, as shown in Figure S8 in the online supplementary material. A contour overview of the compressive strength shown in Figure S9 in the online supplementary material revealed that lower surface strengths formed between the injection and suction wells, particularly in the middle of the sample horizontally. This was true regardless of the injection spacing distance employed. Furthermore, the locations with weaker cementation may have had a decreased prevalence of ureolysis due to fewer bacterial cells. This observation was previously reported by van Paassen (2011).

According to the results of the investigation, samples treated with 214 and 321 mm achieved more homogeneous calcium carbonate distribution, as shown in Figure S8 in the online supplementary material. For well spacings of 10D and 15D, MICP appeared to be more effective in cementing the sand matrix. The 5D sample displayed successful cementation at the central regions of the sand column prior to the placement of the PVC pipes in this location, allowing for a shorter cementation fluid flow network. The reduced distance between the wells guarantees that the soil matrix in the treatment region obtains adequate nutrients. As a result, regardless of the concentration of the cementation reagent, the UCS tends to grow with the number of treatment cycles (Muhammed *et al*., 2021). This eventually results in a higher calcium carbonate content formed within the soil matrix, which contributes to stronger bonding between the soil particles. Regardless of the amount of calcite content within the soil matrix, which may be as low as 1%, it t can influence the soil shear strength and permeability (Montoya and DeJong, 2015). Higher calcium carbonate precipitation has been suggested to occur in a cementation-solution-treated specimen with a shorter treatment cycle and a larger pore volume (Sharma *et al*., 2022; Sharma and Satyam, 2021). Furthermore, the performance of either the injected exogenous or the enhanced native ureolytic bacteria has a strong relationship with the effectiveness of the biocementation (Jiang *et al*., 2022). Because of the negative charge on the cell wall, it is widely assumed that bacterial cells can function as calcium carbonate nucleation sites during the MICP process. Thus, using the push–pull technique will be useful for soil biocementation, particularly involving the injection of exogenous or enriched native ureolytic bacteria alongside the cementation solution.

Despite the positive results of this study, there are a few drawbacks that require more exploration. The flow pattern of the precipitation distribution at the pore scale must be interpreted, particularly when contemplating scale-up of MICP experiments. A comprehensive model study can also be used to examine and optimise the flow patterns in the soil sample. This can be accomplished by scaling up the laboratory size model to gain better knowledge of the MICP process and flow patterns that are applicable in the field. Such simulation studies can also take into account the effects of flow characteristics and treatment longevity for specimens subjected to different MICP injections with varying spacing distances. Another method for studying the cementation flow and ureolysis distribution flow pattern, particularly for large-scale and field-scale MICP experiments, is to utilise non-toxic tracer agents such as sodium bromide and fluorescein. To analyse the transport flow and ureolysis destiny of the cementation in the sand column, these tracers may be injected into the soil during injection as moderate pH buffering agents and colour indicators. Gomez *et al*. (2016b) employed sodium bromide (15 mM) in a 1.7 m dia. tank to study the transport flow of their cementation flow regimes between the three injection wells used for treatment. It is recommended to employ a tracer that has no effect on MICP performance. However, it has been argued that fluorescein might not be a good tracer for soil surface applications. Fluorescein, unlike sodium bromide, has poor tracer qualities when injected into the soil due to its low recovery, pH insensitivity and minimal background interference (Peterson, 2010). MICP researchers have begun to use a passive tracer (sodium bromide) in their field-scale or metre-scale soil biocementation studies (Lee *et al*., 2019b; Nassar *et al*., 2018; San Pablo *et al*., 2020). Ions of the tracer agent can be rinsed out of the soil columns after biocementation treatment by adding deionised water (Lee *et al*., 2019b). More so, the choice of mixing the soil and bacterial suspension before

placing the soil in the mould rather than injecting the soil in the soil column may not be feasible for real field application of an undisturbed soil body. Thus, future work can investigate the influence of this push–pull treatment technique using an injection approach for the bacterial cultures and the cementation solution.

Conclusions

The push–pull injection–suction treatment method was utilised in this study to assess the effect of varied spacings on soil biocementation. The following are the findings of this study.

- *S. pasteurii* cultures and cementation solution (containing 0.75 M urea and calcium chloride) were injected into polystyrene-moulded soil. The findings reveal that variable placements of injection pipes/wells for MICP treatment alter the engineering properties of soil.
- Compressive strength testing revealed that the 15D sample had the greatest values in compressive strength tests (3.42 ± 1.13 and 4.2 ± 2.3 MPa for surface strength and UCS, respectively). The calcium carbonate content distribution was primarily saturated at the bottom layers of the treated soil specimens, while the 15D sample also exhibited the greatest calcium carbonate level.
- The SEM investigation revealed that the 5D sample had the fewest crystal forms and interparticle connections on the soil particles. In 10D and 15D sand particles, large visible chip-like and rhombohedral crystal forms were primarily evident. The findings of this study indicate that the spacings of injection pipes/wells used for soil biocementation can significantly impact the performance of MICP.
- Even though only three injection spacing distances (107, 214 and 321 mm) were used in this study, it was clear that when the injection pipes were used to introduce the cementation solution or bacterial cultures into soil columns, the distances influenced the distribution and formation of calcium carbonate in soil particles. Future field trials on this topic may provide more information about MICP performance when alternative injection spacings are tested.

Acknowledgements

This research was financially supported by Bachy Soletanche (Rueil-Malmaison, France) and the School of Research Office under Swinburne Sarawak Research Grants (SSRG 2-5502).

REFERENCES

Achal V and Pan X (2014) Influence of calcium sources on microbially induced calcium carbonate precipitation by *Bacillus* sp. CR2. *Applied Biochemistry and Biotechnology* **173(1)**: 307–317, https://doi.org/10.1007/s12010-014-0842-1.

Ahenkorah I, Rahman MM, Karim MR and Teasdale PR (2020) A comparison of mechanical responses for microbial- and enzyme-induced cemented sand. *Géotechnique Letters* **10(4)**: 559–567, https://doi.org/10.1680/jgele.20.00061.

Ahenkorah I, Rahman MM, Karim MR and Beecham S (2022) Unconfined compressive strength of MICP and EICP treated sands subjected to cycles of wetting–drying, freezing–thawing and elevated temperature: experimental and EPR modelling. *Journal of Rock Mechanics and Geotechnical Engineering*, https://doi.org/10.1016/j.jrmge.2022.08.007.

Al Imran M, Kimura S, Nakashima K, Evelpidou N and Kawasaki S (2019) Feasibility study of native ureolytic bacteria for biocementation towards coastal erosion protection by MICP method. *Applied Sciences* **9(20)**: article 4462, https://doi.org/10.3390/app9204462.

Al Qabany A, Soga K and Santamarina C (2012) Factors affecting efficiency of microbially induced calcite precipitation. *Journal of Geotechnical and Geoenvironmental Engineering* **138(8)**: 992–1001, https://doi.org/10.1061/(ASCE)GT.1943-5606.0000666.

ASTM (2020) D 2487: Standard practice for classification of soils for engineering purposes (Unified Soil Classification System). ASTM International, West Conshohocken, PA, USA.

Bang SS, Galinat JK and Ramakrishnan V (2001) Calcite precipitation induced by polyurethane-immobilized *Bacillus pasteurii*. *Enzyme and Microbial Technology* **28(4–5)**: 404–409, https://doi.org/10.1016/S0141-0229(00)00348-3.

Bracco LF, Levin GJ, Urtasun N *et al.* (2019) Covalent immobilization of soybean seed hull urease on chitosan mini-spheres and the impact on their properties. *Biocatalysis and Agricultural Biotechnology* **18(4)**: article 101093, https://doi.org/10.1016/j.bcab.2019.101093.

BSI (1990) BS 1377-7:1990: Methods of test for soils for civil engineering purposes. Shear strength tests. BSI, London, UK.

Casas CC, Schaschke CJ, Akunna JC and Jorat ME (2022) Dissolution experiments on dolerite quarry fines at low liquid-to-solid ratio: a source of calcium for MICP. *Environmental Geotechnics* **9(6)**: 331–339, https://doi.org/10.1680/jenge.19.00067.

Chen HJ, Huang YH, Chen CC, Maity JP and Chen CY (2018) Microbial induced calcium carbonate precipitation (MICP) using pig urine as an alternative to industrial urea. *Waste and Biomass Valorization* **10(10)**: 2887–2895, https://doi.org/10.1007/s12649-018-0324-8.

Cheng L and Cord-Ruwisch R (2012) In situ soil cementation with ureolytic bacteria by surface percolation. *Ecological Engineering* **42**: 64–72, https://doi.org/10.1016/j.ecoleng.2012.01.013.

Cheng L and Cord-Ruwisch R (2014) Upscaling effects of soil improvement by microbially induced calcite precipitation by surface percolation. *Geomicrobiology Journal* **31(5)**: 396–406, https://doi.org/10.1080/01490451.2013.836579.

Cheng L, Shahin MA and Cord-Ruwisch R (2017) Surface percolation for soil improvement by biocementation utilizing in situ enriched indigenous aerobic and anaerobic ureolytic soil microorganisms. *Geomicrobiology Journal* **34(6)**: 546–556, https://doi.org/10.1080/01490451.2016.1232766.

Cheng L, Shahin MA and Chu J (2019) Soil bio-cementation using a new one-phase low-pH injection method. *Acta Geotechnica* **14(3)**: 615–626, https://doi.org/10.1007/s11440-018-0738-2.

Choo CS and Ong DEL (2020) Assessment of non-linear rock strength parameters for the estimation of pipe-jacking forces. Part 2. Numerical modeling. *Engineering Geology* **265**: article 105405, https://doi.org/10.1016/j.enggeo.2019.105405.

DeJong JT, Mortensen BM, Martinez BC and Nelson DC (2010) Bio-mediated soil improvement. *Ecological Engineering* **36(2)**: 197–210, https://doi.org/10.1016/j.ecoleng.2008.12.029.

Dhami NK, Reddy MS and Mukherjee A (2016) Significant indicators for biomineralisation in sand of varying grain sizes. *Construction and Building Materials* **104**: 198–207, https://doi.org/10.1016/j.conbuildmat.2015.12.023.

Fang C, He J, Achal V and Plaza G (2019) Tofu wastewater as efficient nutritional source in biocementation for improved mechanical strength of cement mortars. *Geomicrobiology Journal* **36(6)**: 515–521, https://doi.org/10.1080/01490451.2019.1576804.

Feng M, Liu S, Wang J and Hu Y (2020) Influence of stabilisers on the unconfined compressive strength of a fine soil. *Geotechnical Research* **7(4)**: 209–217, https://doi.org/10.1680/jgere.20.00030.

García GM, Márquez GMA, Moreno HCX *et al.* (2016) Characterization of bacterial diversity associated with calcareous deposits and drip-waters, and isolation of calcifying bacteria from two Colombian mines. *Microbiological Research* **182**: 21–30, https://doi.org/10.1016/j.micres.2015.09.006.

Gomez GM, DeJong TJ, Anderson MC, Nelson CD and Graddy MC (2016a) Large-scale bio-cementation improvement of sands. In *Geotechnical and Structural Engineering Congress 2016* (Chandran CY and Hoit MI (eds)). American Society of Civil Engineers, Reston, VA, USA, pp. 941–949.

Gomez MG, Anderson CM, Graddy CMR *et al.* (2016b) Large-scale comparison of bioaugmentation and biostimulation approaches for biocementation of sands. *Journal of Geotechnical and Geoenvironmental Engineering* **143(5)**: 04016124, https://doi.org/10.1061/(ASCE)GT.1943-5606.0001640.

Gowthaman S, Mitsuyama S, Nakashima K, Komatsu M and Kawasaki S (2019) Biogeotechnical approach for slope soil stabilization using locally isolated bacteria and inexpensive low-grade chemicals: a feasibility study on Hokkaido expressway soil, Japan. *Soils and Foundations* **59(2)**: 484–499, https://doi.org/10.1016/j.sandf.2018.12.010.

Gowthaman S, Nakashima K and Kawasaki S (2020) Freeze–thaw durability and shear responses of cemented slope soil treated by microbial induced carbonate precipitation. *Soils and Foundations* **60(4)**: 840–855, https://doi.org/10.1016/j.sandf.2020.05.012.

Gowthaman S, Nakashima K and Kawasaki S (2021) Durability analysis of bio-cemented slope soil under the exposure of acid rain. *Journal of Soils and Sediments* **21(8)**: 2831–2844, https://doi.org/10.1007/s11368-021-02997-w.

Greenberg AE, Clesceri LS and Eaton AD (eds) (1992) *Standard Methods for Examination of Water and Wastewater*, 18th edn. American Public Health Association, Washington, DC, USA.

Hadi S, Abbas H, Almajed A, Binyahya A and Al-Salloum Y (2022) Biocementation by *Sporosarcina pasteurii* ATCC6453 under simulated conditions in sand columns. *Journal of Materials Research and Technology* **18**: 4375–4384, https://doi.org/10.1016/j.jmrt.2022.04.105.

Han Z, Wang J, Zhao H *et al.* (2019) Mechanism of biomineralization induced by *Bacillus subtilis* J2 and characteristics of the biominerals. *Minerals* **9(4)**: 218–244, https://doi.org/10.3390/min9040218.

Harkes MP, van Paassen LA, Booster JL, Whiffin VS and van Loosdrecht MCM (2010) Fixation and distribution of bacterial activity in sand to induce carbonate precipitation for ground reinforcement. *Ecological Engineering* **36(2)**: 112–117, https://doi.org/10.1016/j.ecoleng.2009.01.004.

Jiang NJ, Wang YJ, Chu J *et al.* (2022) Bio-mediated soil improvement: an introspection into processes, materials, characterization and applications. *Soil Use and Management* **38(1)**: 68–93, https://doi.org/10.1111/sum.12736.

Khan YM, Munir H and Anwar Z (2019) Optimization of process variables for enhanced production of urease by indigenous *Aspergillus niger* strains through response surface methodology. *Biocatalysis and Agricultural Biotechnology* **20**: article 101202, https://doi.org/10.1016/j.bcab.2019.101202.

Khui PLN, Rahman MR, Ahmed AS *et al.* (2021) Morphological and thermal properties of composites prepared with poly(lactic acid), poly (ethylene-alt-maleic anhydride), and biochar from microwave-pyrolyzed jatropha seeds. *BioResources* **16(2)**: 3171–3185, https://doi.org/10.15376/biores.16.2.3171-3185.

Lee M, Kolbus CM, Yepez AD and Gomez MG (2019a) Investigating ammonium by-product removal following stimulated ureolytic microbially-induced calcite precipitation. In *Geo-Congress 2019: Soil Improvement* (Meehan CL, Kumar S, Pando MA and Coe JT (eds)). American Society of Civil Engineers, Reston, VA, USA, Geotechnical Special Publication 309, pp. 260–272.

Lee M, Gomez MG, San Pablo ACM *et al.* (2019b) Investigating ammonium by-product removal for ureolytic bio-cementation using meter-scale experiments. *Scientific Reports* **9**: article 18313, https://doi.org/10.1038/s41598-019-54666-1.

Li W, Chen WS, Zhou PP, Cao L and Yu LJ (2013) Influence of initial pH on the precipitation and crystal morphology of calcium carbonate induced by microbial carbonic anhydrase. *Colloids and Surfaces B: Biointerfaces* **102**: 281–287, https://doi.org/10.1016/j.colsurfb.2012.08.042.

Li M, Li L, Ogbonnaya U *et al.* (2015) Influence of fiber addition on mechanical properties of MICP-treated sand. *Journal of Materials in Civil Engineering* **28(4)**: 04015166, https://doi.org/10.1061/(ASCE)MT.1943-5533.0001442.

Li W, Fishman A and Achal V (2021) Ureolytic bacteria from electronic waste area, their biological robustness against potentially toxic elements and underlying mechanisms. *Journal of Environmental Management* **289**: article 112517, https://doi.org/10.1016/j.jenvman.2021.112517.

Lin H, Suleiman MT, Brown DG and Kavazanjian E (2016) Mechanical behavior of sands treated by microbially induced carbonate precipitation. *Journal of Geotechnical and Geoenvironmental Engineering* **142(2)**: 04015066, https://doi.org/10.1061/(ASCE)GT.1943-5606.0001383.

Liu Y, Ong DEL, Oh E, Liu Z and Hughes R (2022) Sustainable cementitious blends for strength enhancement of dredged mud in Queensland, Australia. *Geotechnical Research* **9(2)**: 65–82, https://doi.org/10.1680/jgere.21.00046.

Martinez BC, Dejong JT, Ginn TR *et al.* (2013) Experimental optimization of microbial-induced carbonate precipitation for soil improvement. *Journal of Geotechnical and Geoenvironmental Engineering* **139(4)**: 587–598, https://doi.org/10.1061/(ASCE)GT.1943-5606.0000787.

Mekonnen E, Kebede A, Tafesse T and Tafesse M (2019) Investigation of carbon substrate utilization patterns of three ureolytic bacteria. *Biocatalysis and Agricultural Biotechnology* **22**: article 101429, https://doi.org/10.1016/j.bcab.2019.101429.

Mohsenzadeh A, Aflaki E, Gowthaman S *et al.* (2022) A two-stage treatment process for the management of produced ammonium by-products in ureolytic bio-cementation process. *International Journal of Environmental Science and Technology* **19(1)**: 449–462, https://doi.org/10.1007/s13762-021-03138-z.

Montoya BM and DeJong JT (2015) Stress–strain behavior of sands cemented by microbially induced calcite precipitation. *Journal of Geotechnical and Geoenvironmental Engineering* **141(6)**: 04015019, https://doi.org/10.1061/(ASCE)GT.1943-5606.0001302.

Mortazavi BH, Kariminia T, Shahbodagh B, Rowshanzamir MA and Khoshghalb A (2021) Application of bio-cementation to enhance shear strength parameters of soil–steel interface. *Construction and Building Materials* **294**: article 123470, https://doi.org/10.1016/j.conbuildmat.2021.123470.

Muhammed AS, Kassim KA, Ahmad K *et al.* (2021) Influence of multiple treatment cycles on the strength and microstructure of biocemented sandy soil. *International Journal of Environmental Science and Technology* **18(11)**: 3427–3440, https://doi.org/10.1007/s13762-020-03073-5.

Mujah D, Shahin M and Cheng L (2016) Performance of biocemented sand under various environmental conditions. *Proceedings of the XVIII Brazilian Conference on Soil Mechanics and Geotechnical Engineering (COBRAMSEG 2016), Belo Horizonte, Brazil.*

Mujah D, Shahin MA and Cheng L (2017) State-of-the-art review of biocementation by microbially induced calcite precipitation (MICP) for soil stabilization. *Geomicrobiology Journal* **34(6)**: 524–537, https://doi.org/10.1080/01490451.2016.1225866.

Nandiyanto ABD, Oktiani R and Ragadhita R (2019) How to read and interpret FTIR spectroscope of organic material. *Indonesian Journal of Science and Technology* **4(1)**: 97–118, https://doi.org/10.17509/ijost.v4i1.15806.

Nassar MK, Gurung D, Bastani M *et al.* (2018) Large-scale experiments in microbially induced calcite precipitation (MICP): reactive transport

model development and prediction. *Water Resources Research* **54(1)**: 480–500, https://doi.org/10.1002/2017WR021488.

Ojuri OO, Osagie PO, Oluyemi-Ayibiowu BD *et al.* (2022) Eco-friendly stabilization of highway lateritic soil with cow bone powder admixed lime and plastic granules reinforcement. *Cleaner Waste Systems* **2**: article 100012, https://doi.org/10.1016/j.clwas.2022.100012.

Omoregie AI, Khoshdelnezamiha G, Senian N, Ong DEL and Nissom PM (2017) Experimental optimisation of various cultural conditions on urease activity for isolated *Sporosarcina pasteurii* strains and evaluation of their biocement potentials. *Ecological Engineering* **109**: 65–75, https://doi.org/10.1016/j.ecoleng.2017.09.012.

Omoregie AI, Palombo EA, Ong DEL and Nissom PM (2019) Biocementation of sand by *Sporosarcina pasteurii* strain and technical-grade cementation reagents through surface percolation treatment method. *Construction and Building Materials* **228**: article 116828, https://doi.org/10.1016/j.conbuildmat.2019.116828.

Omoregie AI, Palombo EA and Nissom PM (2021) Bioprecipitation of calcium carbonate mediated by ureolysis: a review. *Environmental Engineering Research* **26(6)**: 200370–200379, https://doi.org/10.4491/eer.2020.379.

Omoregie AI, Muda K, Bakri MK *et al.* (2022) Calcium carbonate bioprecipitation mediated by ureolytic bacteria grown in pelletized organic manure medium. *Biomass Conversion and Biorefinery*, https://doi.org/10.1007/s13399-022-03239-w.

Park GE, Oh HN and Ahn S (2009) Improvement of the ammonia analysis by the phenate method in water and wastewater. *Bulletin of the Korean Chemical Society* **30(9)**: 2032–2038, https://doi.org/10.5012/BKCS.2009.30.9.2032.

Peerun MI, Ong DEL, Choo CS and Cheng WC (2020) Effect of interparticle behavior on the development of soil arching in soil–structure interaction. *Tunnelling and Underground Space Technology* **106**: article 103610, https://doi.org/10.1016/j.tust.2020.103610.

Peng J and Liu Z (2019) Influence of temperature on microbially induced calcium carbonate precipitation for soil treatment. *PLoS ONE* **14(6)**: article e0218396, https://doi.org/10.1371/journal.pone.0218396.

Peterson C (2010) pH dependence and unsuitability of fluorescein dye as a tracer for pesticide mobility studies in acid soil. *Water, Air, & Soil Pollution* **209(1)**: 473–481, https://doi.org/10.1007/s11270-009-0215-5.

Rahman MM, Hora RN, Ahenkorah I *et al.* (2020) State-of-the-art review of microbial-induced calcite precipitation and its sustainability in engineering applications. *Sustainability* **12(15)**: article 6281, https://doi.org/10.3390/su12156281.

San Pablo ACM, Lee M, Graddy CMR *et al.* (2020) Meter-scale biocementation experiments to advance process control and reduce impacts: examining spatial control, ammonium by-product removal, and chemical reductions. *Journal of Geotechnical and Geoenvironmental Engineering* **146(11)**: 04020125, https://doi.org/10.1061/(ASCE)GT.1943-5606.0002377.

Sharma M and Satyam N (2021) Strength and durability of biocemented sands: wetting–drying cycles, ageing effects, and liquefaction resistance. *Geoderma* **402**: article 115359, https://doi.org/10.1016/j.geoderma.2021.115359.

Sharma M, Satyam N and Reddy KR (2022) Liquefaction resistance of biotreated sand before and after exposing to weathering conditions. *Indian Geotechnical Journal* **52(2)**: 328–340, https://doi.org/10.1007/s40098-021-00576-x.

Sidik WS, Canakci H, Kilic IH and Celik F (2014) Applicability of biocementation for organic soil and its effect on permeability. *Geomechanics and Engineering* **7(6)**: 649–663, https://doi.org/10.12989/gae.2014.7.6.649.

Singh AK, Singh M and Verma N (2017) Extraction, purification, kinetic characterization and immobilization of urease from *Bacillus sphaericus* MTCC 5100. *Biocatalysis and Agricultural Biotechnology* **12**: 341–347, https://doi.org/10.1016/j.bcab.2017.10.020.

Soon NW, Lee LM, Khun TC and Ling HS (2014) Factors affecting improvement in engineering properties of residual soil through microbial-induced calcite precipitation. *Journal of Geotechnical and Geoenvironmental Engineering* **140(5)**: 04014006, https://doi.org/10.1061/(ASCE)GT.1943-5606.0001089.

Srivastava S, Bharti RK and Thakur IS (2015) Characterization of bacteria isolated from palaeoproterozoic metasediments for sequestration of carbon dioxide and formation of calcium carbonate. *Environmental Science and Pollution Research International* **22(2)**: 1499–1511, https://doi.org/10.1007/s11356-014-3442-2.

Stocks-Fischer S, Galinat JK and Bang SS (1999) Microbiological precipitation of $CaCO_3$. *Soil Biology and Biochemistry* **31(11)**: 1563–1571, https://doi.org/10.1016/S0038-0717(99)00082-6.

van Paassen LA (2011) Bio-mediated group improvement: from laboratory experiment to pilot applications. In *Geo-frontiers 2011: Advances in Geotechnical Engineering* (Han J and Alzamora DE (eds)). American Society of Civil Engineers, Reston, VA, USA, pp. 4099–4108.

Wang Y, Xu K, Li Y and Feng Q (2015) Fourier transform infrared spectroscopy analysis of the active components in serum of rats treated with Zuogui pill. *Journal of Traditional Chinese Medical Sciences* **2(4)**: 264–269, https://doi.org/10.1016/j.jtcms.2016.01.006.

Wei S, Cui H, Jiang Z *et al.* (2015) Biomineralization processes of calcite induced by bacteria isolated from marine sediments. *Brazilian Journal of Microbiology* **46(2)**: 455–464, https://doi.org/10.1590/S1517-838246220140533.

Whiffin VVS (2004) Microbial CaCO **3** *Precipitation for the Production of Biocement*. PhD thesis, Murdoch University, Perth, Australia.

Whiffin VS, van Paassen LA and Harkes MP (2007) Microbial carbonate precipitation as a soil improvement technique. *Geomicrobiology Journal* **24(5)**: 417–423, https://doi.org/10.1080/01490450701436505.

Xiao JZ, Wei YQ, Cai H *et al.* (2020) Microbial-induced carbonate precipitation for strengthening soft clay. *Advances in Materials Science and Engineering* **2020**: article 8140724, https://doi.org/10.1155/2020/8140724.

Zhao Q, Li L, Li C *et al.* (2014) Factors affecting improvement of engineering properties of MICP-treated soil catalyzed by bacteria and urease. *Journal of Materials in Civil Engineering* **26(12)**: 04014094, https://doi.org/10.1061/(ASCE)MT.1943-5533.0001013.

Zhu X, Li W, Zhan L *et al.* (2016) The large-scale process of microbial carbonate precipitation for nickel remediation from an industrial soil. *Environmental Pollution* **219**: 145–155, https://doi.org/10.1016/j.envpol.2016.10.047.

How can you contribute?

To discuss this paper, please submit up to 500 words to the editor at support@emerald.com. Your contribution will be forwarded to the author(s) for a reply and, if considered appropriate by the editorial board, it will be published as a discussion in a future issue of the journal.

This content has not been peer-reviewed or edited by ICE Publishing.
The accuracy and content of this supplementary file is the sole responsibility of the author.

Supplementary materials

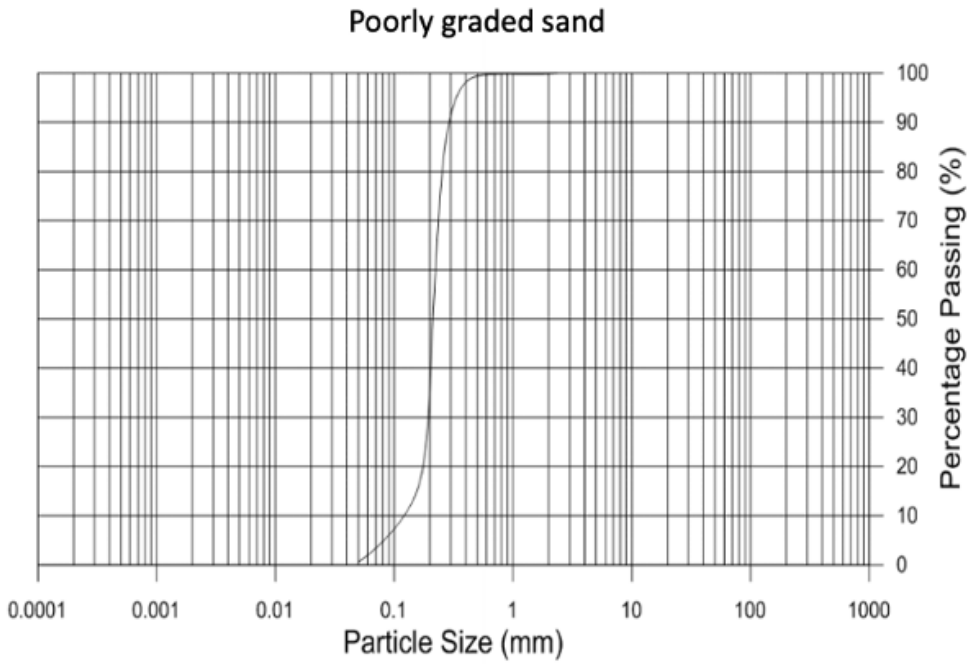

Figure S1: Particle size distribution curve of the poorly graded sand used in this study.

This content has not been peer-reviewed or edited by ICE Publishing.
The accuracy and content of this supplementary file is the sole responsibility of the author.

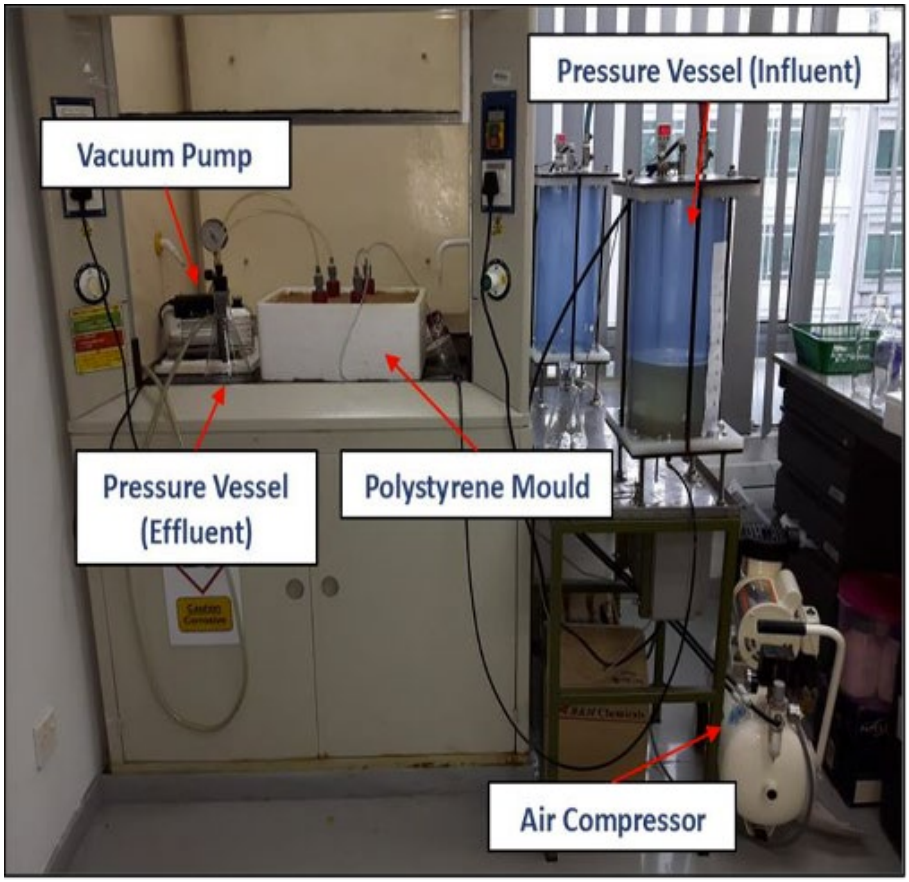

Figure S2: Ureolytic bacterial culture mixed with sand in a portable soil mixer before being transferred to polystyrene mould for biocementation treatment process.

This content has not been peer-reviewed or edited by ICE Publishing.
The accuracy and content of this supplementary file is the sole responsibility of the author.

Figure S3: Conceptual image of the polystyrene box containing four inserted PVC pipes.

This content has not been peer-reviewed or edited by ICE Publishing.
The accuracy and content of this supplementary file is the sole responsibility of the author.

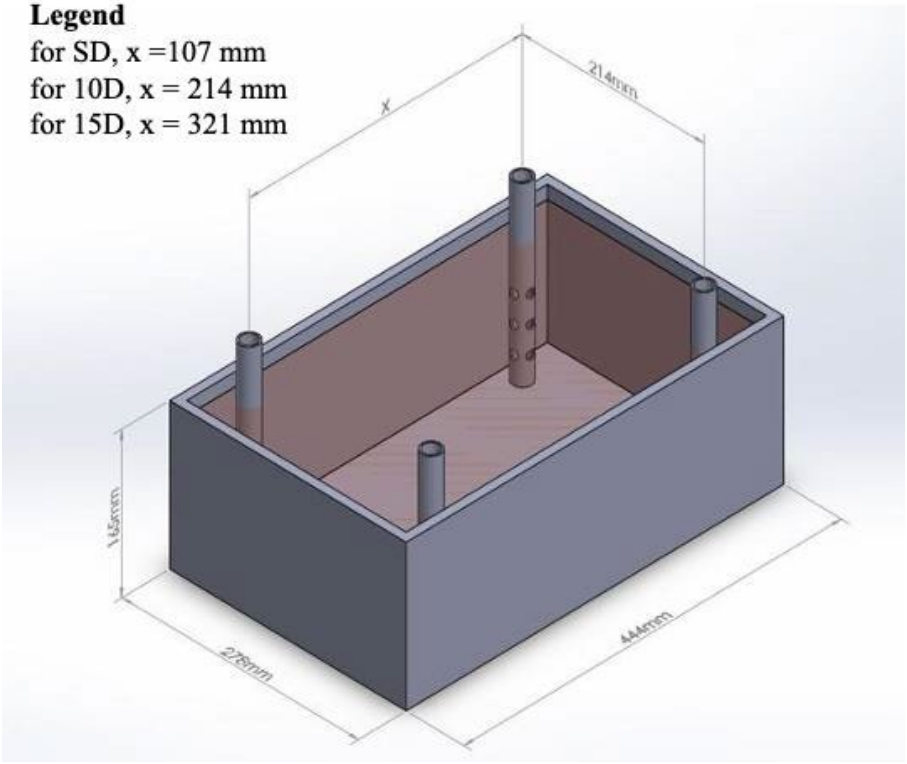

Figure S4: Compacted soil specimen containing rubber pipe insulators around the PVC injection pipes to prevent up-flow of cementation treatment solution and bacterial cultures.

Figure S5: A digital image displaying the two-stage soil biocement injection treatment under laboratory-condition.

This content has not been peer-reviewed or edited by ICE Publishing.
The accuracy and content of this supplementary file is the sole responsibility of the author.

Figure S6: Careful trimming of the core from the biocemented sand specimen for UCS tests.

This content has not been peer-reviewed or edited by ICE Publishing.
The accuracy and content of this supplementary file is the sole responsibility of the author.

Figure S7: Acid wash test of biocemented soil specimens performed in a fume hood.

This content has not been peer-reviewed or edited by ICE Publishing.
The accuracy and content of this supplementary file is the sole responsibility of the author.

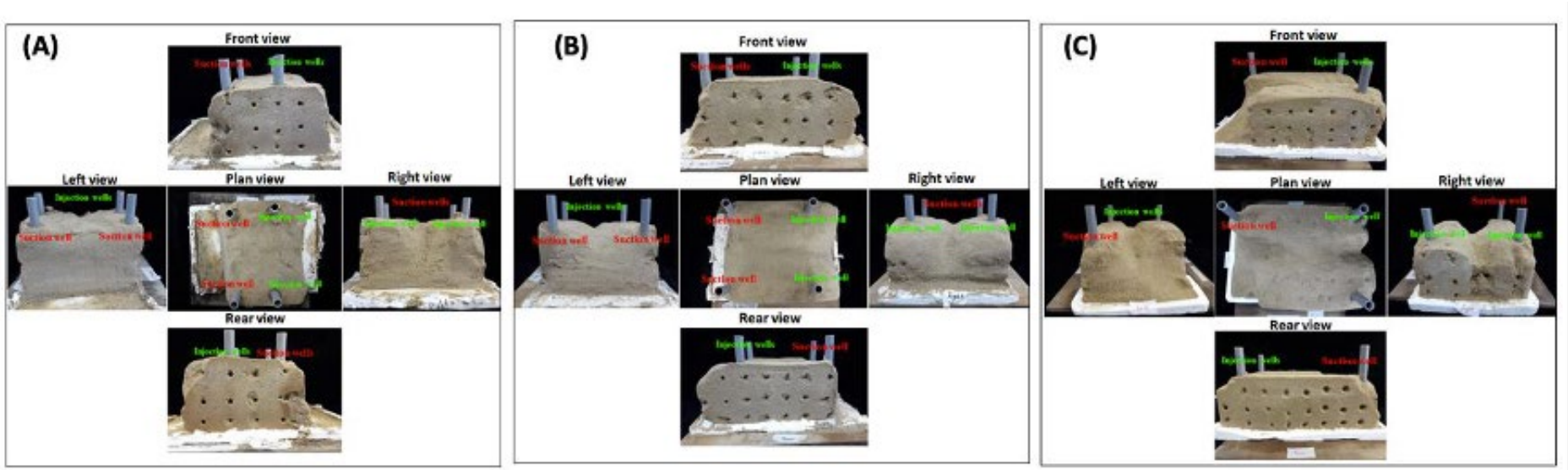

Figure S8: Digital images showing (A) 5D, (B) 10D and (C) 15D biocemented sand specimens that were subjected to surface percolation test.

This content has not been peer-reviewed or edited by ICE Publishing.
The accuracy and content of this supplementary file is the sole responsibility of the author.

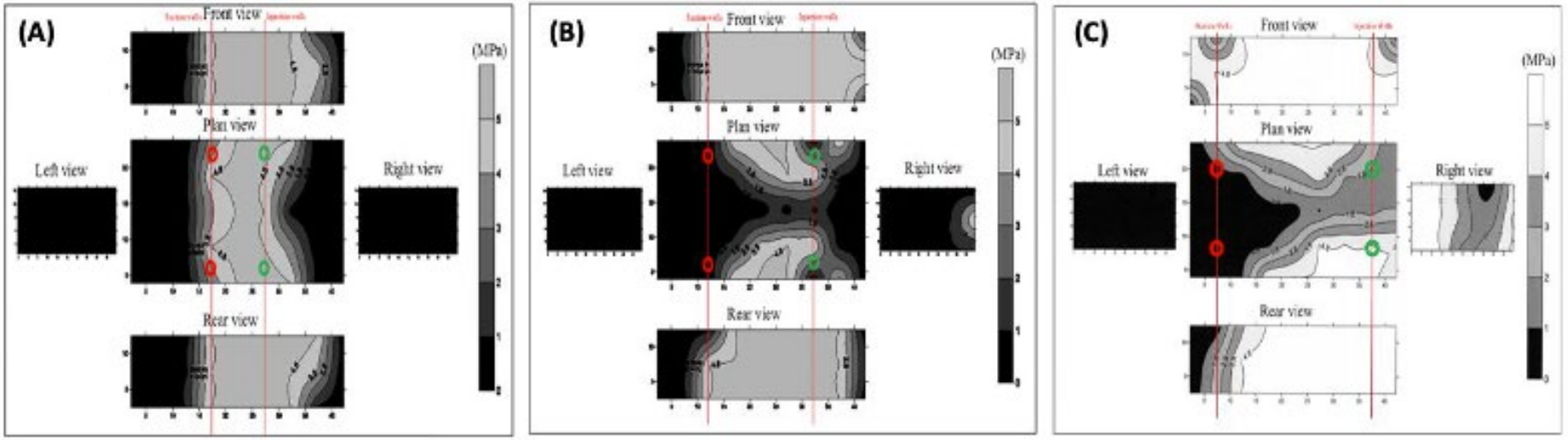

Figure S9: Contour images of surface strength overview for (A) 5D, (B) 10D and (C) 15D biocemented soil specimens after surface percolation test